Nuclear Instruments and Methods in Physics Research A 405 (1998) 525–531

NUCLEAR INSTRUMENTS & METHODS IN PHYSICS RESEARCH Section A

Search for biological objects by refraction radiography using synchrotron radiation of VEPP-3 storage ring

V.S. Gerasimov[a], V.N. Korneev[b,*], G.N. Kulipanov[c], A.A. Manushkin[d], N.A. Mezentsev[c], V.F. Pindyurin[c], P.M. Sergienko[a], V.A. Somenkov[d], M.A. Sheromov[c], S.Sh. Shilstein[d], A.A. Vazina[a]

[a]*Institute of Theoretical and Experimental Biophysics, 142292 Moscow region, Pushchino, Russia*
[b]*Institute of Cell Biophysics, 142292 Moscow region, Pushchino, Russia*
[c]*Budker Institute of Nuclear Physics, 630090 Novosibirsk, Russia*
[d]*Russian Research Center, Kurchatov Institute, 123182 Moscow, Russia*

Abstract

The possibility of using synchrotron radiation (SR) for obtaining the X-ray images of biological objects by the method of refraction radiography at the energies of 8.9 and 33.2 keV is shown. The results of experiments at the storage ring VEPP-3 (Novosibirsk) are presented. In comparison with a conventional X-ray source, the exposition time with SR is reduced by a factor of more than a thousand (approximately, down to 1–2 s), and the quality of images is improved.

1. Introduction

The search for the internal structure of the object by using penetrating radiation (electromagnetic, ultrasonic etc.) is based on local changes in the intensity of radiation after its interaction with a substance. The features with the sizes from one to ten micrometers (small organs, blood vessels, the cells in tissues etc.) must be differentiated in the study of internal structure of biological objects. It is impossible to perform by ultrasonic diagnostic, NMR-technique, or exposure to a hard X-ray radiation (of quantum energy $E > 5$ keV) because of the comparatively weak interaction of the radiation types with organic substances. However, just this fact allows us to expose the objects of up to ten centimeters in size to radiation. In X-ray medical diagnostics, the features as small as a 1 mm cannot be revealed even with the use of computer tomography, special contrasting or other means. The features smaller than a 1 μm in size can be observed by using soft X-rays, but this radiation acts strongly on organic substances. Therefore, it is only suitable for structure investigation of thin cuts of tissue. The majority of biological tissues are opaque to visible light, and, when usual light microscopes are employed for investigations, we are forced to work with slices because only exterior surfaces are seen. Thus, to reveal small features of inner structure of the object by penetrating radiation, we need not use absorption, but other processes accompanied interaction of radiation with a substance.

Recently, the methods for object imaging by the hard X-ray radiation were developed which were based on refraction and interference processes, in addition to absorption. In the refraction method (refraction radiography), the images are formed using X-ray beams refracted in the object at certain angles [1–4]. To register the refracted X-ray beams, two- and three-crystal spectrometers with perfect crystals are used. The required angular resolution is provided by the proper choice of reflections from the crystal planes, and, if necessary, the parts of microradian can be obtained. The possibility of observing the features of biological objects with the sizes down to 10–20 μm at the exposition time of tens of minutes has been demonstrated in known works [1–4]. However, it was noted that the large vertical divergence of the X-ray tube beam influences on the image quality.

Another method of the image formation is based on interference of the rays passed through adjacent regions of objects. The coherent synchrotron radiation (SR) of the ESRF source with a divergence of several microradians in both directions is used [5,6]. In this method, named by its authors as "phasecontrast microradiography", the image is obtained due to interference, and the angular resolution is provided by very strong collimation of the SR beam. The features smaller than one micrometer are observed on these images at the exposition time of about a second. The limitation for the method is in a necessity for using a unique SR source.

* Corresponding author. E-mail: korneev@ibfk.nifhi.ac.ru

0168-9002/98/$19.00
PII S0168-9002(98)00004-7

The aim of the present work is to develop the method of refraction radiography of biological objects with SR from the VEPP-3 storage ring (INP, Novosibirsk) and to compare its possibilities with those using radiation from an X-ray tube.

2. The technique of the experiment

The angle of deflection of X-rays on the phase boundary is determined by the jump of the refractive index Δn and the glancing angle α [2]:

$$\Delta\alpha = \Delta n \operatorname{ctg} \alpha . \quad (1)$$

For the boundary between air and a substance with the index of refraction n, the jump is equal to:

$$\Delta n = (1 - n) = \lambda^2 N r \rho f_0 / (2\pi A) , \quad (2)$$

where λ is wavelength, N is Avogadro number, r is classical electron radius, ρ is density, f_0 ($\approx Z$) is atomic factor of scattering at zero angle, Z is atomic number, and A is atomic weight.

For water and organic substances, the ratio $\rho Z/A \approx$ const, and, taking the data for water and $\lambda = 0.15$ nm, we will have $(1 - n) \approx 4 \times 10^{-6}$. Consequently, to observe interior and exterior surfaces in biological objects at $\alpha \leqslant \approx 45°$, the angular resolution of about several microradians is needed in accordance with the expression (1). In refraction radiography with characteristic radiation of the Cu-anode X-ray tube ($\lambda = 0.154$ nm), such resolution was achieved by using sequential Bragg reflections (333) on two parallel Si crystals and by placing the specimen between these crystals [2].

In the experiments on Sr, to avoid difficulties connected with keeping separate crystals in the parallel position, we used the channel-cut silicon crystal with the reflection planes (511). The crystal has the same Bragg angle and angular resolution as Si(333). The images were obtained using nonrefracted radiation that is similar to the method of "light field" in light microscopy. Thus, in the experiments on SR, the conditions being analogous with those of [2], were essentially reproduced.

These experiments were carried out at two experimental stations of the storage ring VEPP-3: the station of small-angle diffractometry, described in [7], with the photon energy $E = 8.9$ keV ($\lambda = 0.15$ nm), and the station of subtraction angiography with the energy $E = 33.2$ keV ($\lambda = 0.04$ nm).

Schematic layout of the experimental setup at the small-angle diffractometry station is presented in Fig. 1. Formation of the SR beam was performed in the median plane by means of two crystals. The first crystal-monochromator (Ge(111), asymmetry coefficient is about 0.3) was located at a distance 17 m from the SR emission point and formed, at $\lambda = 0.15$ nm, the parallel X-ray beam due to bending the

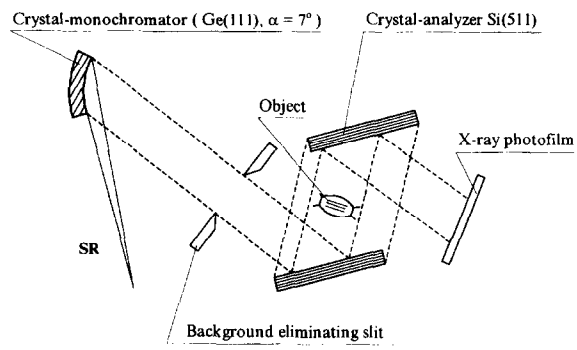

Fig. 1. Schematic layout of the refraction imaging experiments on the SR beam with a quantum energy 8.9 keV.

monochromator surface in the form of logarithmic cylinder. The second crystal Si(511) was used as analyzer, and was cut from the monolithic block of silicon with two parallel symmetrical diffraction surfaces separated by a 15 mm slot. The angular resolution was $\omega \approx 15$ μrad. Background radiation was eliminated by means of special slit installed ahead of the crystal-analyzer. The object was placed between the surfaces of the crystal-analyzer by such a way that only the X-rays, diffracted from the first surface of the crystal, passed through the object. Images of the object were registered by the X-ray photofilm RM-1.

Deflection of radiation by the object in the horizontal plane causes the formation of refraction radiogram of the object, i.e. the shadow image of its refracting surfaces. At the same time, the absorption contrast on the refraction radiogram remains. In the discussed scheme, the full horizontal divergence and the natural vertical collimation of the SR beam are used. The sizes of the beam, incident on the crystal-monochromator, and the diffracted X-ray beam in the plane of the object were 2×9 mm^2 and 5×9 mm^2, respectively. Thus, the angular resolution was determined by double Bragg reflection on the channel-cut crystal Si(511). The vertical divergence of the SR beam is smaller by a factor of two orders in comparison with one for radiation from the X-ray tube (≈ 0.03 radian).

The spectral resolution $(\Delta\lambda/\lambda)_1$ of the monochromator is determined by the value of horizontal divergence ϵ_h of the incident beam:

$$(\Delta\lambda/\lambda)_1 = \epsilon_h / tg\ \theta_1 \approx 4 \times 10^{-4} . \quad (3)$$

The dispersion broadening $\Delta\theta_d = (\Delta\lambda/\lambda)_1$ $(tg\theta_1 - tg\ \theta_2) \approx 370$ μrad is arisen under sequential reflecting from Ge(111) ($tg\ \theta_1 = 0.24$) and Si(511) ($tg\ \theta_2 = 0.93$).

When the angular resolution is ω, the spectral resolution on the specimen is

$$(\Delta\lambda/\lambda)_2 = (\Delta\lambda/\lambda)_1 (\omega/\Delta\theta_d) = 2 \times 10^{-5} . \quad (4)$$

We see that it is better by a factor of 10 than that at using the X-ray tube when spectral resolution in X-ray refraction

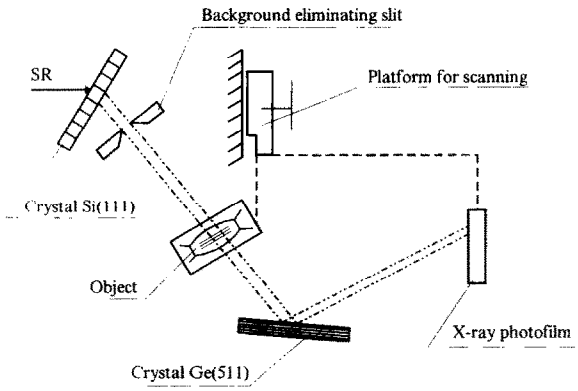

Fig. 2. Schematic layout of the refraction imaging experiments on the SR beam with a quantum energy 33.2 keV.

radiography is determined by the width of the emitted characteristic lines.

Thus, the difference between the conditions of obtaining refraction radiograms using SR against using the X-ray tube is the stronger collimation and higher monochromatization of radiation.

The experimental setup on the station of digital subtraction angiography is schematically shown in Fig. 2. Formation of the SR beam was realized by means of two separate crystals with a 6 m distance between them, and by the background eliminating slit. The first crystal Si(111) monochromated the SR beam in Laue-geometry and directed it downwards at 7.5° to the horizontal plane. The second crystal Ge(511) (symmetrical) was used as the analyzer. The object was placed before the crystal-analyzer, and registration of the object images was performed onto the X-ray photofilm. The size of the beam in the plane of the object was $0.5 \times 37\ mm^2$. To obtain the images of extended objects (with the sizes of larger than 0.5 mm), we carried out their scanning. For this aim the object and the photofilm were installed on the platform, which allowed them to simultaneously move across the beam at the given velocity.

3. Experimental results

The refraction images, obtained using the experimental layout of Fig. 1, are presented on Figs. 3–7. On the images of insects (Fig. 3a–e), the details of various organs are visualized. For example, on the image of the bug *Anobium pertinax*, the smallest details of chitin cover are clearly discernible. We clearly see a cover of the body and the wings on the image of the bug *Scolytidae*. The image of the mosquito *Culicidae* displays the internal cavities (Fig. 3c). The boundaries of the bodies and internal organs are distinctly and clearly drawn on the radiograms of the ant *Formicidae* (Fig. 3d) and the cockroach *Blatta orientalis* (Fig. 3e). On the image of the maple seed (*Acer platanoides*), the smallest veins are seen (Fig. 4a). The needles of the pine *Pinus sylvestris* clearly show fibrous structure (Fig. 4b). Furthermore, collagen filaments extracted from a tail of the rat *Rattus*, as well as in threads of polyethylene and batiste fabric are also visualized on the radiograms (Figs. 5a–c).

The images of the frog organs (*Ranidae esculenta*) demonstrate the structure of soft tissues (Fig. 6b–c), as well as the structure of bones (Fig. 6a). Though the absorption in the bones is much stronger, the soft tissues on the refraction radiograms are also well distinguished. The smallest discernible details have the sizes of about 30 μm, that is close to the spatial resolution of the X-ray film. We note the high contrast of the image of air bubble in Fig. 6(b).

The refraction images of biological objects in the presented scheme of the experiment with the use of SR are obtained for the time of about one second. Similar images of the same objects with the use of the X-ray tube can be acquired for the time of about 30 minutes. It was demonstrated in the X-ray experiments that, for the same wavelength, the features of sizes smaller than one millimeter are practically invisible without a high angular resolution. Therefore, the structural details in biological objects, which are invisible at usual absorption X-ray radiography, can be easily observed using SR. In the prospect, when the exposure time will be reduced to the fractions of a second, the observation of small animals can be possible not only *in vitro* but *in vivo*, as well. The quality of refraction images on SR is better than the obtained one for similar objects by using conventional X-ray tubes in the analogous scheme of experiments.

In refraction radiography with the X-ray tube radiation, the high angular resolution is realized only in the scattering plane, and, as a consequence, the horizontal interfaces in the object remain nearly invisible since the angle deflections of the rays are perpendicular to the scattering plane. The similar anisotropy is also observed on the refraction images obtained with SR. For example, on the image of Fig. 6(b), the contrast of vertical boundaries between soft tissues and air is very high, while the similar horizontal boundaries are imperceptible. The strong difference in contrast is also observed for vertical and for tilted boundaries of the air bubble in Fig. 6(b). To demonstrate the contrast anistropy, the radiogram of the model object–the polyethylene capillary with water and two air bubbles–was taken (Fig. 7). We see that the width of area of high contrast for vertical boundaries air–polyethylene and for low contrast meniscus air–water differs very much, while the refraction index jump on these boundaries is distinguished only a little [2]. We note that the interface water–polyethylene does not give the refraction contrast due to small angle deflection or radiation on this surface in comparison with the used angular resolution. Nevertheless, the boundaries of such types which are the models for

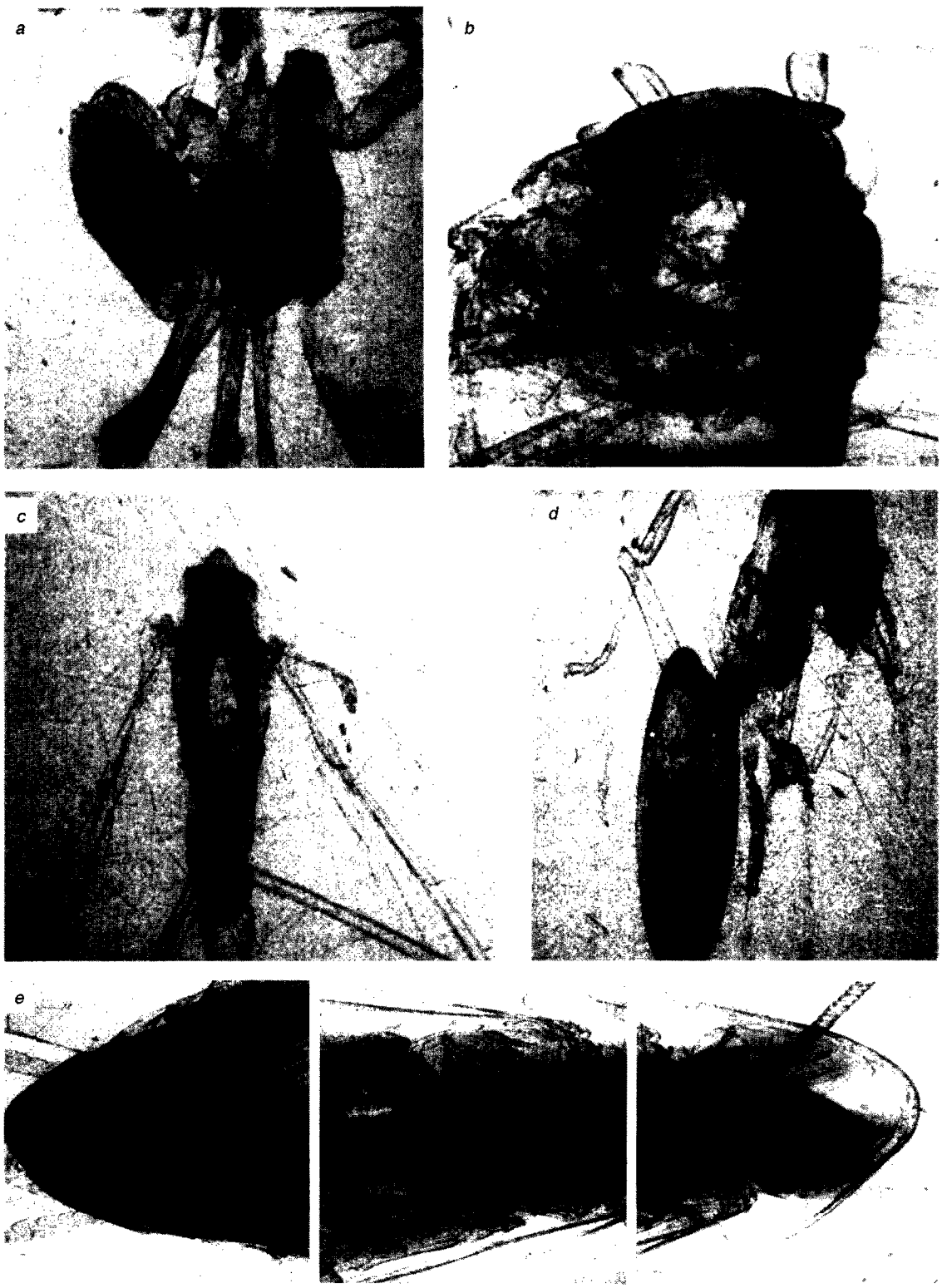

Fig. 3. Images of insects: (a) bug *Anobium pertinax*; (b) bug *Scolytidae*; (c) mosquito *Culcidae*; (d) ant *Formicidae*; (e) cockroach *Blatte orientalis* (three fragments).

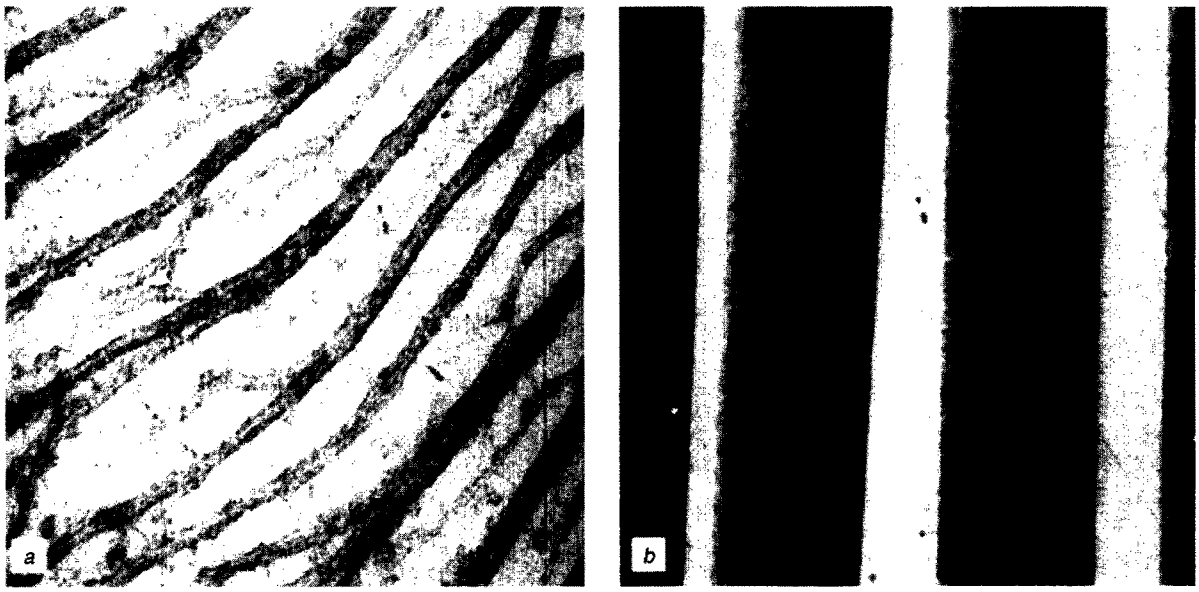

Fig. 4. Images of plant organs: (a) wing of seed of the maple *Acer platanoides*; (b) needles of the pine *Pinus sylvestris*.

interfaces between the tissues of close composition, can be observed at higher angular resolution.

In the experiments while using the layout of Fig. 2, the contrast of the edges of the polyethylene tube walls was obtained. The edges of copper wire by which the sample was hung, had contrastingly less clear outlines. It is likely in this case that the contrast image of the sample had occurred mainly through the process of refraction, while the image of the copper wire was formed as a result of the absorption phenomena.

4. Discussion

On the SR refraction images of the biological objects, the small details of their structure revealed whose sizes came near to the resolution of the X-ray film. We evaluated the spatial resolution Δa_γ of refraction radiography on the SR beam in approximation of geometrical optics. We then proceed from effective horizontal divergence γ of the beam on the object and the distance R between the object and the film:

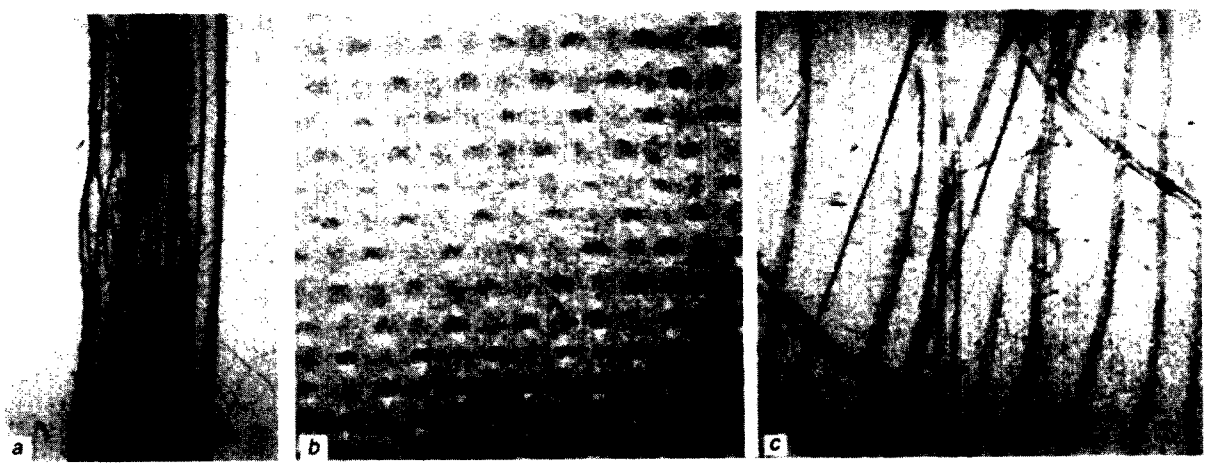

Fig. 5. Images of fibrous structure: (a) collagen filaments extracted from a tail of the rat *Rattus*; (b) batiste fabric; (c) threads of polyethylene.

Fig. 6. Images of frog organs (*Ranidae esculenta*): (a) foreleg; (b) heart (two fragments); (c) eye (fragment).

$$\Delta a_\gamma = \gamma R . \tag{5}$$

The γ value is determined by spectral resolution (in the chosen experimental scheme $\Delta\lambda/\lambda \approx 2 \times 10^{-5}$), and is about 15 μrad. At $R \approx 3$ cm, this gives, according to the formula (5), the value Δa_γ to be about 0.5 μm, which is far outside the real resolution of the photofilm. Another evaluation is based on the fact that the image of each point of the object is blurred by the value being equal to the penetration depth of radiation into the crystal-analyzer. This, so called, "depth of extinction" t, according to [9] is:

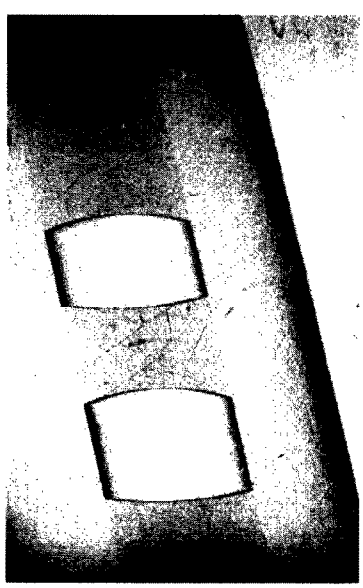

Fig. 7. Polyethylene capillary with water and air bubbles.

$$t = \lambda \sin\theta(\pi\chi) , \tag{6}$$

where θ is the Bragg angle and χ is the Fourier-component of polarization (for the chosen wavelength and reflection $\chi = 4.5 \times 10^{-6}$). This evaluation gives for our experimental conditions the value Δa_γ to be about 3 μm. Thereby, the spatial resolution of refraction radiograms on SR must be near 3 μm. It means that the spatial resolution of the obtained images can be substantially improved by using other photomaterial, for instance, nuclear photoplates.

In conclusion, we note that the presented results demonstrate the possibility of obtaining the high-quality images of biological objects with a spatial resolution of about several micrometers when using such SR sources as the VEPP-3. Combination of high angular resolution in the horizontal plane with the natural small divergence of the beam in the vertical plane allows us, to maximal extent, to utilize the SR advantages. It may be argued that, on this basis, it will be possible to examine the alive objects and even to shoot the X-ray refraction cinema. The needed consideration for this is the reduction of an exposure in several times only, bringing it down to a value of less than 1/16 s, that seems to be possible at the modern level of the technique.

References

[1] E. Foerster, K. Goetz and P. Zaumseil, Kristall Technik 15 (1980) 937.

[2] V.A. Somenkov, A.K. Tkalich and S.Sh. Shilstein, Sov. Phys. Tech. Phys. 36(11) (1991) 1309.

[3] E.A. Beliaevskaya, V.N. Ingal and P.V. Petrashen, Abst. 2nd European Symp. "X-ray Topography and High Resolution Diffraction", Berlin, September 1994, p. 44.

[4] T.J. Davis, D. Gao, T.E. Gureyev, A.W. Stevenson and W. Wilkins, Nature 373 (1995) 595.
[5] A. Snigirev, I. Snigireva, V. Kohn, S. Kuznetsov and I. Schelokov, Rev. Sci. Instr. 66(12) (1995) 5486.
[6] P. Cloetens, R. Barret, J. Baruchel, J.-P. Guigau and M.J. Schlenker, Phys. D 29 (1996) 133.
[7] V.M. Aul'chenko, S.E. Baru, A.M. Gadzhiev, V.S. Gerasimov, V.N. Korneev, P.M. Sergienko, M.A. Sheromov, A.A. Vazina and M.B. Yasenev, Nucl. Instr. and Meth. A 359 (1995) 216.
[8] A.A. Manushkin, N.L. Mitrofanov, K.M. Podurets, V.A. Somenkov and S.Sh. Shilstein, Preprint RRC Kurchatov Inst. IAE-5791/10 (1994).
[9] Z.G. Pinsker, Dynamical Scattering of X-Rays in Crystals (Springer, Heidelberg, 1984).